Proc. Natl. Acad. Sci. USA
Vol. 86, pp. 4382–4386, June 1989
Biochemistry

Mammalian aspartate transcarbamylase (ATCase): Sequence of the ATCase domain and interdomain linker in the CAD multifunctional polypeptide and properties of the isolated domain

(pyrimidine biosynthesis/protein domains/nucleotide sequence/carbamoyl-phosphate synthetase/dihydroorotase)

JAMES P. SIMMER, RUTH E. KELLY*, JOSHUA L. SCULLY, DENNIS R. GRAYSON†, AUSTIN G. RINKER, JR., SANDRA T. BERGH, AND DAVID R. EVANS

Department of Biochemistry, Wayne State University, Detroit, MI 48201

Communicated by William N. Lipscomb, March 2, 1989

ABSTRACT **Mammalian aspartate transcarbamylase (ATCase; carbamoyl-phosphate:L-aspartate carbamoyltransferase, EC 2.1.3.2) is part of a 240-kDa multifunctional polypeptide called CAD, which also has carbamoyl-phosphate synthetase and dihydroorotase activities. We have sequenced selected restriction fragments of a Syrian hamster CAD cDNA that are clearly homologous to three prokaryotic ATCases. These studies, combined with previous sequence data, showed that the ATCase domain of CAD is encoded by 924 base pairs and has a mass of 34,323 Da and a pI of 9.8. While the bacterial pyrimidine biosynthetic enzymes are separate proteins, in mammals the ATCase domain is fused to the carboxyl end of the CAD chimera via a 133-amino acid (14-kDa) linker with an unusual amino acid composition, a pI of 10.2, and pronounced hydrophilic character. The fully active domain isolated from proteolytic digests was characterized by partial amino acid sequencing and amino acid analysis. Trypsin cleavage produced the ATCase domain with a 20-residue amino-terminal extension. Hydrodynamic studies showed that the isolated domain is a 110-kDa trimer with a Stokes radius of 41 Å. The mammalian ATCase domain and the prokaryotic enzymes have virtually identical active-site residues and are likely to have the same tertiary fold.**

Aspartate transcarbamylase (ATCase, EC 2.1.3.2) catalyzes the formation of *N*-carbamoyl-L-aspartate from carbamoyl phosphate and L-aspartate in the *de novo* pyrimidine biosynthetic pathway. *Escherichia coli* ATCase, an allosteric enzyme (1, 2), is a 303-kDa molecule that can be dissociated into two catalytic trimers and three regulatory dimers (3–6). Lipscomb and his associates (7–9) have determined the three-dimensional structure of *E. coli* ATCase in both R ("relaxed") and T ("taut") allosteric conformations. *Bacillus subtilis* ATCase, a trimer of 34-kDa catalytic chains that lacks regulatory chains, resembles the isolated *E. coli* ATCase catalytic trimer (10). Lerner and Switzer (11) sequenced the *B. subtilis* ATCase gene and showed that it is homologous to the *E. coli* catalytic chain.

The structural organization of mammalian ATCase is distinctly different. The ATCase activity is carried by a domain of a 240-kDa multifunctional polypeptide (12–14). This protein, called CAD, also has carbamoyl-phosphate synthetase (CPSase II, EC 6.3.5.5) and dihydroorotase (DHOase, EC 3.5.2.3) activities. In mammals CPSase II is an allosteric enzyme, whereas ATCase is unregulated (15). Controlled proteolysis of CAD isolated from an overproducing hamster cell line releases a 40-kDa fragment having ATCase activity, which Grayson and Evans (16) purified from elastase digests. The isolated ATCase domain exists as a stable, homogeneous oligomer with kinetic properties very similar to those of the parent molecule.

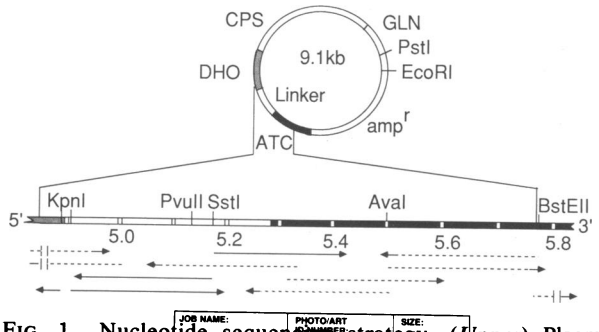

FIG. 1. Nucleotide sequencing strategy. (*Upper*) Plasmid pCAD142 contains a cDNA insert encoding the glutamine-binding domain (GLN), the CPSase domain (CPS), the DHOase domain (DHO), the DHOase–ATCase linker, and the ATCase domain (ATC) of CAD. The ampicillin-resistance (amp^r) marker for selection of bacterial transformants is also shown. (*Lower*) The region of pCAD142 sequenced is shown schematically: ATCase domain, black bar; ATCase–DHOase linker, open bar; and DHOase domain, stippled bar. Relevant restriction sites and distance (kb) from the start of the cDNA insert are shown. Sequencing reactions were primed with the M13 universal primer (solid arrows) or with synthetic oligonucleotides (dashed arrows).

Shigesada *et al.* (17) constructed a nearly full-length hamster CAD cDNA clone and sequenced about 500 base pairs (bp) at the 3′ end of the molecule. On the basis of homology with the *E. coli* catalytic subunit and complementation of a *pyrB*-deficient strain, they concluded that this region encodes the ATCase domain, which is therefore located on the carboxyl end of the polypeptide. The mammalian ATCase domain has recently been detected by enzyme and immunochemical assays in extracts of *E. coli* transformed with subcloned fragments of the 3′ end of pCAD142 (18).

In this study we present the DNA sequence extending from the 3′ end of the DHOase coding region to the known ATCase sequence.‡ The deduced amino acid sequence corresponds to the polar domain of the hamster ATCase and the 14-kDa linker that connects the DHOase and ATCase domains. We also report additional characterization of the ATCase domain isolated from controlled proteolytic digests of CAD.

The publication costs of this article were defrayed in part by page charge payment. This article must therefore be hereby marked "*advertisement*" in accordance with 18 U.S.C. §1734 solely to indicate this fact.

Abbreviations: ATCase, aspartate transcarbamylase; CPSase, carbamoyl-phosphate synthetase; DHOase, dihydroorotase; CAD, a polypeptide having CPSase, ATCase, and DHOase activities.

*Present address: Gene Expression Laboratory, Salk Institute, La Jolla, CA 92037.
†Present address: Fidia-Georgetown Institute for the Neurosciences, Georgetown Medical School, Washington, DC 20007.

‡The sequence reported in this paper has been deposited in the GenBank data base (accession no. M23652).

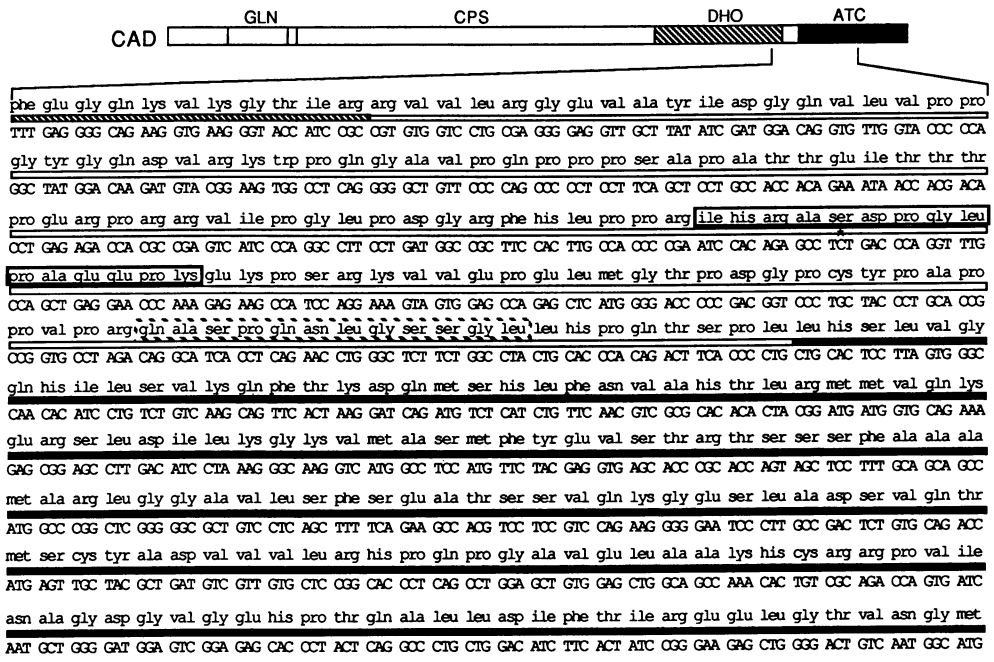

FIG. 2. Nucleotide sequence and deduced amino acid sequence of the extreme carboxyl end of the DHOase domain (hatched bar), the linker (open bar), and the amino half of the ATCase domain. The carboxyl half of the ATCase domain, which has already been sequenced (17), is not included. Protein sequence data for phosphorylation site 2 (27) serine (≛) and peptide (boxed) and the amino end of the tryptic ATCase domain (boxed, broken lines) are also shown.

MATERIALS AND METHODS

The plasmid pCAD142 contained a 6.5-kilobase (kb) insert including most of the CAD cDNA (17). The DNA sequence was determined by the dideoxy method of Sanger *et al.* (19). DNA template was produced by subcloning restriction fragments (Fig. 1) into pBS(+) and isolating packaged single-stranded DNA from transformed, VCSM13-infected XL1-Blue cells (Stratagene). The BIONET program FASTP was used for pairwise alignment of amino acid sequences, with the optimal final alignment by small shifts of insertions and deletions. Hydropathy plots [Kyte and Doolittle scale (20)] and secondary-structure profiles (21) were calculated by using BIONET. Molecular weights and pI values were calculated by using the IBI sequence analysis programs.

CAD was isolated from hamster cell line 165-23, kindly provided by George Stark (Imperial Cancer Research Fund, London), as described previously (14). The ATCase domain generated by controlled proteolysis with elastase or trypsin (protein/protease weight ratio, 100) was isolated on a CM-Sephadex column (16) and its purity was checked by SDS/PAGE (22) and by assaying ATCase activity (23). A Waters Pico-Tag system with precolumn phenyl isothiocyanate derivatization (24) was used for amino acid analysis. Automated Edman degradation was performed on a gas-phase sequenator. The molecular weight and Stokes radius were determined by gel filtration (25) on a calibrated Sephadex G-200 column.

RESULTS

The nucleotide sequence of a region that maps from about 4.8 to 5.8 kb of the 6.5-kb cDNA insert of pCAD142 (Fig. 2) was determined. We also confirmed the published sequence (17), which extends 456 nucleotides further downstream to the stop codon. We sequenced all of this region but not both strands. Our data agreed with the published sequence except that we found a guanine instead of an adenine in the third position of the codon for Gln-240 in CAD (see Fig. 3); this discrepancy does not change the amino acid sequence.

Table 1. Comparison of CAD ATCase domain with homologous proteins

	Hm ATC	Ec ATC	St ATC	Bs ATC	Rt OTC
Hm ATC		138	135	102	79
Ec ATC	44		287	105	79
St ATC	43	92		99	77
Bs ATC	32	34	31		75
Rt OTC	25	24	24	23	

Upper half of the matrix gives number of amino acid identities; lower half gives percent identities based on the common length of the pair. References and abbreviations are given in Fig. 3 legend.

Identification and Characterization of the ATCase Domain. The segment of the mammalian protein encoded by this region of the insert of plasmid pCAD142 was clearly homologous to three prokaryotic ATCases. The alignment of the deduced amino acid sequences (Fig. 3)§ was achieved with few insertions and deletions and gave identities ranging from 32% to 44% (Table 1). The first amino acid of the mammalian ATCase domain was coincident with the amino terminus (excluding the terminal methionine) of the *E. coli* catalytic subunit. Thus the domain is encoded by 924 bp near the 3′ end of pCAD142. This sequence codes for 308 residues of the polypeptide chain with a molecular weight of 34,323. In a similar fashion we identified the location and boundaries of the DHOase domain (unpublished data). The sequence that spans the region between the carboxyl end of the DHOase domain and the amino end of the ATCase domain codes for a 133-amino acid interdomain connecting peptide, or linker. One of two sites phosphorylated by cAMP-dependent kinase (27) was found in the linker region.

Grayson and Evans (16) isolated a fragment from proteolytic digests that carries the ATCase activity of CAD. SDS/PAGE showed that the isolated ATCase domain generated by elastase digestion had a molecular weight of 40,000, while that of the domain isolated from trypsin digests was about 500 higher. We have now found by Edman degradation (unpublished data) that the amino end of the tryptic fragment maps to the trypsin site in the linker closest to the ATCase domain (Fig. 2). Thus the isolated domain has a 20-residue extension

§Regions of the ATCase domain that are well conserved throughout phylogeny differ in the published sequence (26) of *Drosophila melanogaster* CAD. These differences can be reconciled by small shifts in the reading frame. Although reading frame 3 was published, frame 2 reads DSIKVVSSYADVVV (amino acids 90–103) and PLINAG (123–128), and frame 1 reads GDLKNGRTVHSL (161–172) and LPDTDVLYMTRI (219–230).

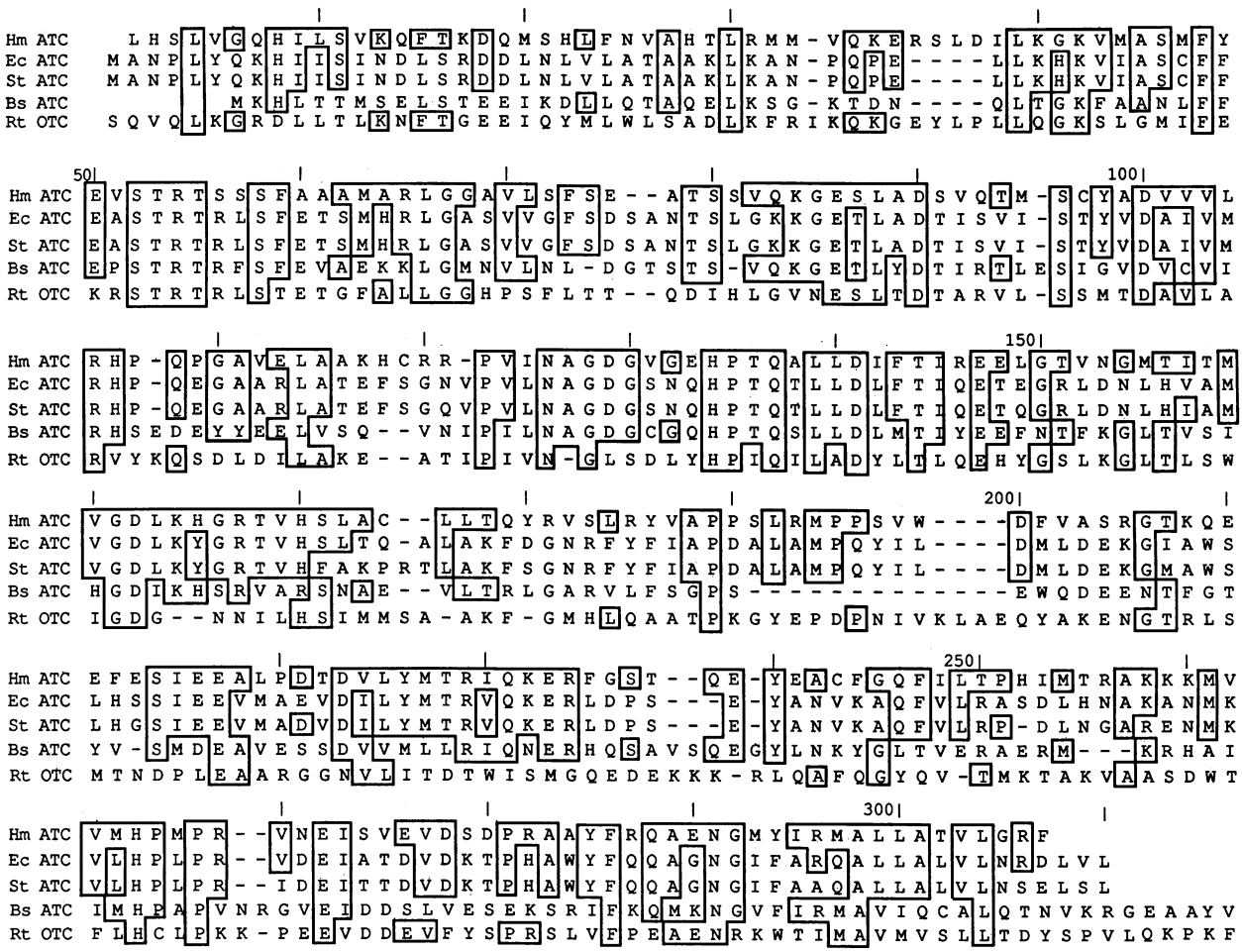

FIG. 3. Alignment of ATCase and ornithine transcarbamylase amino acid sequences. The hamster CAD ATCase domain [Hm ATC (ref. 17 and this report)] is shown aligned with ATCase from *E. coli* [Ec ATC (28, 29)], *Salmonella typhimurium* [St ATC (30)], and *B. subtilis* [Bs ATC (11)] as well as ornithine transcarbamylase from rat [Rt OTC (31)]. Three residues (ISH) have been omitted from the carboxyl end of Bs ATC.

on the amino terminus. The molecular weight of the domain plus the amino-terminal extension was calculated to be 36,249. This value is about 10% lower than the observed value. Isoelectric focusing of the isolated domain gave a pI of 9.4 (16), close to the value of 9.8 calculated from the amino acid sequence. The amino acid composition of the isolated domain was similar to that calculated from the sequence (Table 2). Except for histidine and methionine, which gave erratic, low values, the average difference between the observed and deduced composition was 7%.

The oligomeric structure of the isolated domain determined by gel filtration (Fig. 4) showed that the undenatured protein had a molecular weight of 112,000 and a Stokes radius of 41.8 Å. The Stokes radius combined with the sedimentation coefficient determined previously (16) gave a molecular

Table 2. Calculated and observed composition of domain

Amino acid	No. of residues		Amino acid	No. of residues	
	Calc.	Obs.*		Calc.	Obs.*
Ala	27	28.8	Thr	21	21.4
Val	29	29.8	Tyr	8	8.6
Leu	31	31.8	Asx	18	16.6
Ile	12	12.4	Glx	36	32.5
Pro	16	20.4	Lys	13	11.8
Met	17	10.8	Arg	21	23.7
Phe	13	12.4	His	12	7.6
Gly	20	25.4	Cys	4	2.5
Ser	29	28.8	Trp	1	ND†

*Isolated tryptic ATCase domain. Total number of residues is 328.
†Not determined.

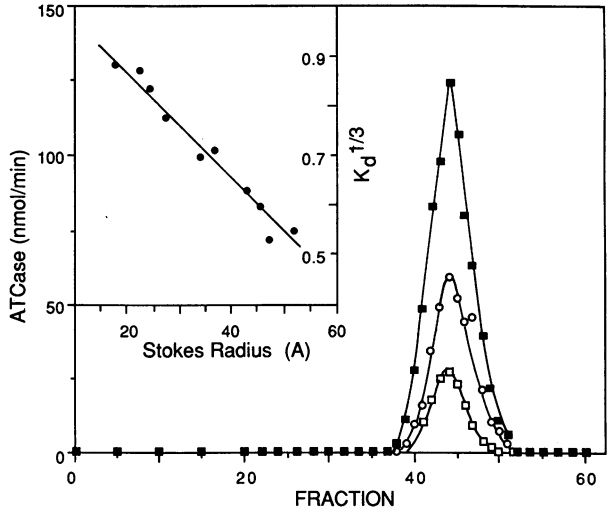

FIG. 4. Stokes radius of the isolated ATCase domain, determined by gel filtration at three different initial protein concentrations: 70 (□), 200 (○), and 390 (■) μg/ml. (*Inset*) Standard curve obtained by chromatography of 10 proteins of known Stokes radius (32, 33).

weight of 109,000. A trimer of M_r 36,300 polypeptides would have a molecular weight of 108,900. Gel filtration carried out at three concentrations of the domain gave superimposable elution profiles indicating that the subunit structure was stable in this range. The frictional ratio is typical of globular proteins. The chemical and hydrodynamic properties predicted for a protein encoded by the nucleotide sequence of the putative ATCase domain are similar to those exhibited by the proteolytic fragment known to account for all of the ATCase activity of CAD (Table 3).

Comparison of Mammalian and Prokaryotic ATCases. A comparison of the functional and structural properties of the mammalian domain with two well-characterized prokaryotic ATCases (Table 3) indicates that these proteins are very similar. The ATCase domain of CAD, the *E. coli* ATCase catalytic subunit, and the *B. subtilis* ATCase are all trimers of M_r 34,000 polypeptides having comparable kinetic parameters and no regulatory control.

The primary structures of these proteins are also highly homologous. The *E. coli* catalytic chain and the mammalian domain were found to be 44% identical with only two insertions and three deletions in the CAD sequence. This degree of sequence homology strongly suggests that the tertiary folds of the mammalian and bacterial proteins are basically the same. The structural homology was also reflected in similar hydrophilic profiles (Fig. 5).

Table 3. Comparison of the hamster CAD ATCase domain, *E. coli* ATCase catalytic subunit, and *B. subtilis* ATCase

Property	Hamster*	*E. coli*†	*B. subtilis*‡
Molecular weight (M_r)			
Domain, obs.		33,000	33,500
Domain, calc.	34,323	33,943	34,185
Fragment, obs.	40,500		
Fragment, calc.	36,249		
No. of residues			
Domain	308	310	304
Fragment	328		
Isoelectric point			
Domain, calc.	9.8	6.2	6.0
Fragment, obs.	9.4		
Fragment, calc.	9.8		
Sedimentation coefficient			
Domain, obs.		6.0	5.4
Fragment, obs.	6.2		
Stokes radius			
Domain, obs.		39.5	45.7
Fragment, obs.	41.8		
Trimer M_r			
Domain, obs.		100,000	102,000
Domain, calc.	103,044	101,829	102,555
Fragment, obs.§	110,800		
Fragment, calc.	108,747		
Frictional ratio¶	1.32		
K_m			
Carbamoyl phosphate (μM)	20.7	14.0	110
Aspartate (mM)	21.3	20.7	7.0
Turnover number (sec^{-1})	80	253	217
pH optimum	8.5	8.5	8.5

Calculated values are based on the deduced sequence. Domain refers to the prokaryotic monomers or the CAD ATCase domain.
*Observed isoelectric point (pI), sedimentation coefficient ($s_{20,w}$), and all kinetic parameters except pH optimum are from ref. 16; other data are from this study.
†Sequence data (28, 29); kinetic data (34); other properties (3, 6).
‡Structural properties and kinetic data (10); sequence data (11).
§Average of values obtained by gel filtration (M_r 112,600), by centrifugation (M_r 110,700) and by calculation (35) from Stokes radius and $s_{20,w}$ (M_r 109,000).
¶Calculated as described (35) by using the partial specific volume derived (36) from the amino acid composition.

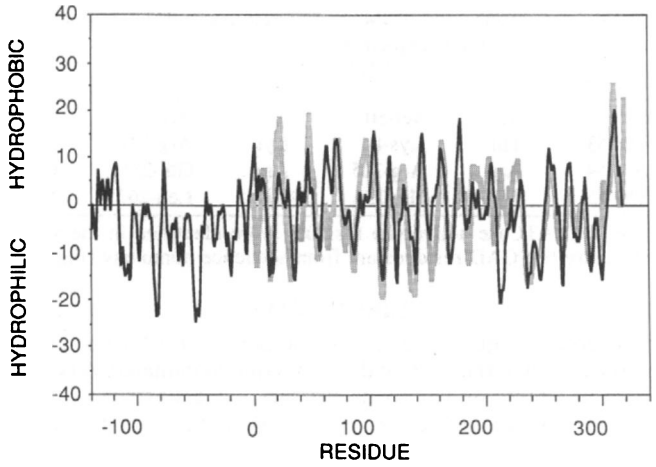

FIG. 5. Hydropathy plot of the ATCase domain and interdomain linker (solid line) aligned with the *E. coli* ATCase catalytic chain (stippled line). Numbering begins with the first residue of ATCase, so the linker residues are designated by negative numbers.

Assuming that the mammalian domain and the *E. coli* catalytic chain have similar tertiary structures, all of the insertions and deletions mapped to the surface of the monomer and occurred outside regions of well-defined secondary structure (Fig. 6). The sole exception was a single amino acid deletion in an α-helix at position 183. The residues involved in substrate binding and catalysis in the *E. coli* enzyme (7–9) were found to be conserved in the CAD sequence (Table 4). The only difference was that Leu-267 has been replaced by methionine in CAD, but this interaction involves the backbone amide group, not the side chain.

Analysis of the Interdomain Connecting Chain Segment. The 133-amino acid linker that connects the ATCase and DHOase domains had a calculated molecular weight of 14,282. In addition to its extraordinary size, the linker had a very unusual amino acid composition consisting of 28 prolines (21%), 31 charged residues (23%), and many small and hydroxy amino acids. The hydropathic profile showed that this region is very hydrophilic (Fig. 6), while secondary-structure calculations (not shown) predicted a high frequency of reverse turns and little propensity to form helical or sheet structures. Thus the linker appeared to be an exposed chain segment on the surface of the molecule.

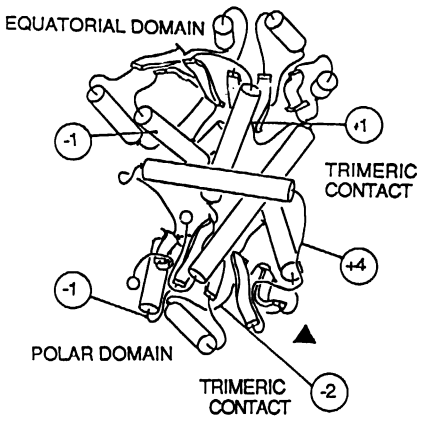

FIG. 6. Insertions and deletion in the CAD ATCase domain. The tertiary fold of *E. coli* catalytic chains, based on the x-ray structure determined by Lipscomb and coworkers (7–9), is shown with the numbers representing insertions (positive) or deletions (negative) in the CAD sequence. (Figure adapted from ref. 7 with permission.)

Table 4. Conservation of the *E. coli* active-site residues in the CAD ATCase domain sequence

E. coli	CAD	*E. coli*	CAD	*E. coli*	CAD
Ser-52	Ser	Ser-80	Ser	Arg-167	Arg
Thr-53	Thr	Lys-84	Lys	Arg-229	Arg
Arg-54	Arg	Arg-105	Arg	Gln-231	Gln
Thr-55	Thr	His-134	His	Leu-267	Met

E. coli ATCase active-site residues were identified in the x-ray structure (9); CAD residues are from sequence homology (Fig. 3).

DISCUSSION

Nucleotide sequence analysis combined with further characterization of the protein disclosed that mammalian ATCase is remarkably similar to its prokaryotic counterparts. The mammalian domain and *E. coli* catalytic chain are the same size (34 kDa), share 44% amino acid sequence identity, and have nearly superimposable hydropathic profiles. Edman degradation of the isolated domain precisely defined its amino terminus, while the hydrodynamic studies established that it associates into compactly folded trimers. The virtual identity of active-site residues and the similarity in kinetic parameters suggest that the *E. coli* and CAD enzymes have similar catalytic mechanisms. A trimeric structure is required for the activity of the *E. coli* enzyme because the active site is composed of residues from adjacent polypeptide chains (catalytic subunits C1 and C2) (8, 37). We conclude that the ATCase domain in CAD must associate as trimers and thus participate in the formation of the higher oligomers (10, 38).

Only 52% (27 of 52) of the residues involved in the *E. coli* trimeric (C1–C2) contacts (7–9) are conserved in the CAD sequence, suggesting that significant remodeling of this interface has occurred, perhaps as a result of the loss of allosteric control in the mammalian enzyme. Of the 25 C1–C2 residues not conserved in CAD, 20 are also different in *B. subtilis* ATCase, which like the CAD ATCase domain is a trimeric, unregulated enzyme.

The ATCase and DHOase domains are connected by a 133-residue chain segment that is highly susceptible to proteases. In addition to elastase and trypsin, we found that five other proteases cleave the linker first, although the size of the resulting ATCase domain varies somewhat (data not shown). On the basis of differences in the sizes of the fragments produced by trypsin and *Staphylococcus aureus* V8 protease, Rumsby *et al.* (39) estimated that the protease-sensitive region might be as large as 100 amino acids, a value close to that found in the sequencing study.

The isolated ATCase and DHOase domains are fully active even though most of the connecting chain segment has been removed during the proteolytic digestion (18, 40). It is therefore unlikely that the linker is required for catalysis. Allosteric control persists long after the proteolytic cleavage of the ATCase and DHOase domains, so that the allosteric ligands probably do not bind in this region of the molecule. Phosphorylation site 2 was thought by Carrey *et al.* (27) to be less critical to regulation than site 1. Its location in the linker region, far from the regulated CPSase domain in a highly accessible region ideal for adventitious reaction with the kinase, supports this interpretation. [Carrey and Hardie (41) correctly identified the location of phosphorylation site 1 but were uncertain of the location of site 2. Sequence analysis shows that site 2 is in the DHOase–ATCase linker and probably corresponds to the minor phosphorylation site 3 postulated by those authors.]

An intriguing possibility is that the linker may be important for the metabolic compartmentation of intermediates (42). A long interdomain chain segment may be necessary to bring the CPSase and ATCase domains, located at opposite ends of the polypeptide, into close proximity. The linker is long enough to span the 100-Å monomer (38), while the hydropathic and secondary-structure calculations suggest an extended structure exposed to the solvent. Both the ATCase domain (unlike the bacterial enzymes) and the linker have very high isoelectric points (9.8 and 10.4, respectively), indicating that they carry a strong positive charge that may favor ionic interactions with the more acidic DHOase and CPSase domains.

We thank Drs. George Stark (Imperial Cancer Research Fund, London) and Jeffrey Davidson (University of Kentucky) for pCAD142, Hyesook Kim for Edman sequence analysis, and Hong Wan, Grace Hannon, and Kathleen Benoit for expert assistance. Work was supported by National Cancer Institute Grants CA27674 and T32 CA09531 (J.P.S.). Protein sequence determination and amino acid analysis were done at the Wayne State Macromolecular Core Facility.

1. Yates, R. A. & Pardee, A. B. (1956) *J. Biol. Chem.* **221**, 757–770.
2. Gerhart, J. C. & Pardee, A. B. (1962) *J. Biol. Chem.* **237**, 891–896.
3. Gerhart, J. C. & Schachman, H. K. (1965) *Biochemistry* **4**, 1054–1062.
4. Wiley, D. C. & Lipscomb, W. N. (1968) *Nature (London)* **218**, 1119–1121.
5. Weber, K. (1968) *Nature (London)* **218**, 1116–1119.
6. Rosenbusch, J. P. & Weber, K. (1971) *J. Biol. Chem.* **246**, 1644–1657.
7. Krause, K. L., Volz, K. W. & Lipscomb, W. N. (1987) *J. Mol. Biol.* **193**, 527–553.
8. Kim, K. H., Pan, Z., Honzatko, R. B., Ke, H.-M. & Lipscomb, W. N. (1987) *J. Mol. Biol.* **196**, 853–875.
9. Ke, H., Lipscomb, W. N., Cho, Y. & Honzatko, R. B. (1988) *J. Mol. Biol.* **204**, 725–746.
10. Barbson, J. S. & Switzer, R. L. (1975) *J. Biol. Chem.* **250**, 8664–8669.
11. Lerner, C. G. & Switzer, R. L. (1986) *J. Biol. Chem.* **264**, 11156–11165.
12. Shoaf, W. T. & Jones, M. E. (1973) *Biochemistry* **12**, 4039–4051.
13. Mori, M., Ishida, H. & Tatibana, M. (1975) *Biochemistry* **14**, 2622–2630.
14. Coleman, P. F., Suttle, D. P. & Stark, G. R. (1977) *J. Biol. Chem.* **252**, 6378–6385.
15. Tatibana, M. & Shigesada, K. (1972) *J. Biochem. (Tokyo)* **72**, 549–560.
16. Grayson, D. R. & Evans, D. R. (1983) *J. Biol. Chem.* **258**, 4123–4129.
17. Shigesada, K., Stark, G. R., Maley, J. A., Niswander, L. A. & Davidson, J. N. (1985) *Mol. Cell. Biol.* **175**, 1–7.
18. Maley, J. A. & Davidson, J. N. (1988) *Mol. Gen. Genet.* **213**, 278–284.
19. Sanger, F., Nicklen, S. & Coulson, A. R. (1977) *Proc. Natl. Acad. Sci. USA* **74**, 5463–5467.
20. Kyte, J. & Doolittle, R. F. (1982) *J. Mol. Biol.* **157**, 105–132.
21. Chou, P. Y. & Fasman, G. D. (1974) *Biochemistry* **13**, 222–245.
22. Laemmli, U. K. (1970) *Nature (London)* **227**, 680–685.
23. Mally, M. I., Grayson, D. R. & Evans, D. R. (1980) *J. Biol. Chem.* **255**, 11372–11380.
24. Bidlingmeyer, B. A., Cohen, S. A. & Tarvin, T. L. (1984) *J. Chromatogr.* **336**, 93–104.
25. Ackers, G. K. (1964) *Biochemistry* **3**, 723–730.
26. Freund, J. N. & Jarry, B. P. (1987) *J. Mol. Biol.* **193**, 1–13.
27. Carrey, E. A., Campbell, D. G. & Hardie, D. G. (1985) *EMBO J.* **4**, 3735–3742.
28. Schachman, H. K., Pauza, C. D., Navre, M., Karels, M. J., Wu, L. & Yang, Y. R. (1984) *Proc. Natl. Acad. Sci. USA* **81**, 115–119.
29. Hoover, T. A., Roof, W. D., Foltermann, K. F., O'Donovan, G. A., Bencini, D. A. & Wild, J. R. (1983) *Proc. Natl. Acad. Sci. USA* **80**, 2462–2466.
30. Michaels, G., Kelln, R. A. & Nargang, F. E. (1987) *Eur. J. Biochem.* **166**, 55–61.
31. Takiguchi, M., Miura, S., Mori, M., Tatibana, M., Nagata, S. & Kaziro, Y. (1984) *Proc. Natl. Acad. Sci. USA* **81**, 7412–7416.
32. Porath, J. (1963) *Pure Appl. Chem.* **6**, 233–244.
33. Ackers, G. K. (1975) in *The Proteins*, eds. Neurath, H., Hill, R. L. & Roeder, C. L. (Academic, New York), 3rd Ed., Vol. 1, pp. 1–94.
34. Porter, R. W., Modebe, M. O. & Stark, G. R. (1969) *J. Biol. Chem.* **244**, 1846–1859.
35. Siegel, L. M. & Monty, K. J. (1969) *Biochim. Biophys. Acta* **112**, 346–362.
36. Cohn, E. J. & Edsall, J. T., eds. (1943) in *Proteins, Amino Acids and Peptides* (Reinhold, New York), pp. 370–381.
37. Robey, E. A. & Schachman, H. K. (1985) *Proc. Natl. Acad. Sci. USA* **82**, 361–365.
38. Lee, L., Kelly, R. E., Pastra-Landis, S. C. & Evans, D. R. (1985) *Proc. Natl. Acad. Sci. USA* **82**, 6802–6808.
39. Rumsby, P. C., Campbell, P. C., Niswander, L. A. & Davidson, J. N. (1984) *Biochem. J.* **217**, 435–440.
40. Kelly, R. E., Mally, M. I. & Evans, D. R. (1986) *J. Biol. Chem.* **261**, 6073–6083.
41. Carrey, E.A. & Hardie, D.G. (1988) *Eur. J. Biochem.* **171**, 583–588.
42. Christopherson, R. I. & Jones, M. E. (1980) *J. Biol. Chem.* **255**, 11381–11395.